IMPACT OF PETROPHYSICAL PROPERTIES ON HYDRAULIC FRACTURE ANALYSIS

Seals, Kelsey and Engler, Thomas, New Mexico Institute of Mining and Technology

This paper was prepared for presentation at the SPWLA 58th Annual Logging Symposium held in Oklahoma City, Oklahoma, USA, June 17-21, 2017.

ABSTRACT

Defining petrophysical and mechanical properties of target and barrier zones are key components of the hydraulic fracture modeling process; subsequently, the selection of the detail necessary to accurately model fracture/reservoir performance is challenging. This work investigates whether using detailed petrophysical and mechanical properties provides fracture design parameters that better represent actual fracture behavior and subsequent well performance than a single-layered model.

The approach was to model an existing hydraulic fracture treatment and well performance from a well located in the northern Delaware Basin producing from the lower Brushy Canyon Formation. Models varied from a single layer model with simple-averaged, petrophysical properties to a fine resolution 1-ft model with detailed petrophysical values. Detailed core descriptions were constructed to appropriately represent the thin-bedded and micro-laminated sandstones and siltstones.

In addition, point load tests measured values of fracture toughness for specific lithofacies from 600 to 1100 psi-in½. In comparison, the default value for a sandstone system is 1000 psi-in½. Other mechanical properties, e.g., Poisson's ratio and Young's modulus were derived from well logs, and were within typical values.

For the fracture modeling phase, the actual treatment volumes, rates and pressures were inputted into the model along with the measured petrophysical and mechanical properties. Model net pressure was matched with the actual values to verify the output. The dimensionless fracture conductivity (FCD) from the various models ranged from 4.8 to 13.6. The range depends on the variation of lithofacies included in the fine resolution models and their associated mechanical/petrophysical properties. Adding micro-laminated and bioturbated siltstones at the expense of clean sandstone in the finer resolution models resulted in higher permeability, fracture toughness and lower stress gradient.

For the production history matching phase, simulation pressures were significantly overestimated compared to actual measured bottomhole pressures for all single layer models regardless if actual or default mechanical properties were used. The overestimation reflects a threefold increase in pore volume due to the single layer values. For the finer resolution 1-ft model, the simulation pressure was significantly below measured pressure values using default mechanical properties. However, using actual mechanical properties in the 1-ft resolution model resulted in an increase in the FCD due to the decrease in fracture toughness and stress gradient input values. As a result, a very good match was obtained between simulation and actual pressures; indicating the 1-ft model with the measured mechanical properties is a good representation of the actual reservoir system.

INTRODUCTION

In oil and gas operations, the completion process is one of the most critical components in drilling and producing a successful well. Hydraulic fracturing is one of the most common completion or "stimulation" methods used in medium and low-permeability reservoirs. It is also a costly investment, comprising 50% or more of drilling and completion budget per well (U.S. Department of Energy, 2016). A successful stimulation can increase the rate of return (ROI), ultimate recovery, and overall productivity over the life of the well, while an unsuccessful or poorly-designed stimulation can have the opposite effect, resulting in potentially severe economic losses. Accurate reservoir representation in hydraulic fracture modeling is a critical component for effective stimulations, yet complete and detailed input data is frequently limited.

As an example, the use of limited and simplified reservoir data for treatment designs is inadequate for complex, highly-laminated reservoirs such as the Brushy Canyon Formation in the Delaware Basin. The focus of this work is to determine if using detailed reservoir rock properties provides fracture design parameters that better represent the actual fracture behavior and subsequent well performance.

BRUSHY CANYON FORMATION, DELAWARE BASIN

Renewed exploration and development efforts in the Brushy Canyon Formation since the 1990s have spurred the need for effective completion treatment designs to account for the multilayered reservoirs and potential fracture propagation into water-bearing zones. Given these challenges and complexities, consideration of numerous lamination sequences and variable rock and reservoir properties is key for accurately modeling hydraulic fracture behavior. Vertical variations in porosity, permeability, and lithologies, combined with the proximity of water-bearing zones to hydrocarbon-bearing zones characterize the complex nature of the formation, proving challenging for modeling fracture treatment designs. Many Delaware Basin fracturing treatments did not adequately account for the formation's laminated sand-silt sequences and variations in reservoir properties, and as a result, many wells are plagued with poor hydrocarbon recovery and high water production (Scott & Carrasco, 1996).

The #23 well was selected for use in this work, and is located in the Nash Draw field in southeast New Mexico. The well was drilled and completed in the Lower Brushy Canyon Member of the Delaware Mountain Group (Guadalupian). Well #23 and the surrounding Nash Draw field have been well-studied, with numerous data sources available for designing and simulating hydraulic fracture treatments. This data includes core analysis, mechanical properties log, direct rock properties measurements from point-load tests, Micro Imaging logs, and traditional well logs.

WORKFLOW

The approach is to use an existing treatment and model the fracture behavior using both detailed properties and simplistic properties using hydraulic fracture software. The simplistic geologic properties consist of a single layer with average porosity and permeability values, and default values for mechanical properties included in the software. The detailed geologic properties, including porosity, permeability, fracture toughness, and rock mechanical properties, were derived from well logs, point load tests, and core analysis. Lithologic, petrophysical, and mechanical properties were selected for investigations since these parameters have the highest degree of uncertainty. Hydraulic fracture treatment parameters such as proppants and fluids were not varied from the original treatment. The results from the fracture analysis including were used to model the actual well performance of the subject well. The workflow diagram is shown in figure 1.

Fig. 1 Workflow diagram outlining the methods and procedures used in this work.

Core Descriptions. Approximately 130' of core for the #23 was used to collect data including rock descriptions, measurements, and photographs. This data was also used to create digitized core schematics. The thirteen boxes of ~3-in wide slabbed core were loaned for use in this work by the New Mexico Bureau of Geology and Mineral Resources' Core Library facility. Each core slab was measured and described according to changes in lithology, color, fracture locations, and sedimentary structures. Details of core descriptions and measurements can be found in Seals, 2016.

Core Schematics. Core schematics (Fig. 2) are digital representations of the core on a 1:4 scale. The core was digitized from depths 6650'-6780' using photographs and measurements from the core descriptions. The schematics were created for simplified visualization of the detailed and complex features of the lower Brushy Canyon. More

importantly, the schematics display the locations and behavior of numerous preferential fractures. The diagrams include depth locations of 35 of the 41 perforations along the wellbore and the core samples taken for use in the point load test. The core schematics were used extensively in this work, proving valuable for correlating RA tracer log data with preferential fracture locations, and allowed for enhanced visualization of the mechanical properties log data.

Fig 2. Core schematic (right) was created for simplified digital visualization of the detailed and complex features in the #23 core. Preferential fracture shown in core photos (left).

Log Analysis. Water saturation values (S_W) from the core analysis were compared to log-derived S_W values (Figure 3). The S_W core and log data correlate reasonably well, indicating that both the log-derived or core-derived source data are appropriate for use in reservoir and fracture modeling applications.

Point Load Test Sample Selection. To acquire fracture toughness values direct measurements were taken using the point load test method. From the core descriptions and schematics, six different lithofacies were selected for testing (Table 1). This work followed the methods for sample selection and testing procedures as suggested by the International Society for Rock Mechanics (ISRM) Commission on Testing Methods publication (Franklin, 1985). Rock specimens can be in the shape of either cut blocks, core, or irregular lumps. Due to size and shape constraints of the core from the #23 well, the test samples were cut into blocks and tested accordingly.

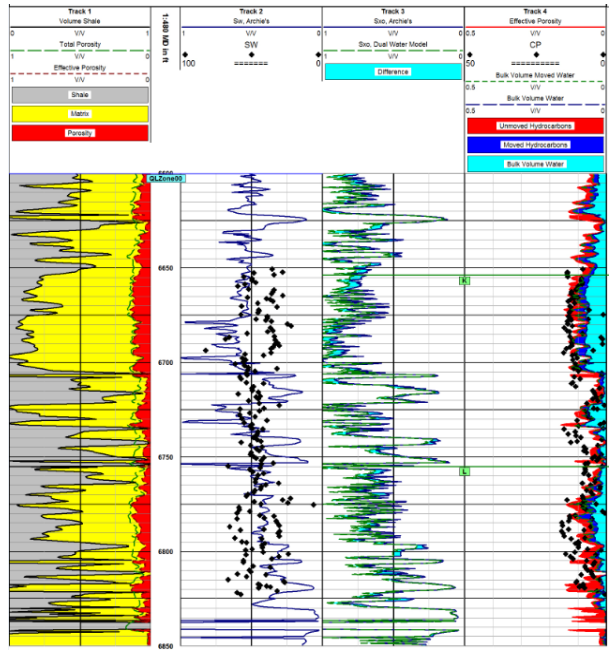

Fig. 3 Results from the log evaluation of #23 well. Track 2 (second from left) shows log-derived Sw values (blue line) and core-derived Sw values (black diamonds). Top of perforated K and L sands are denoted with green markers and lines in Track 3 and 4, 6654' and 6755', respectively.

Depth (ft)	Lithology
6652'	Sandstone (clean, structureless)
6718'	Laminated silt (medium gray)
6738'	Bioturbated sandstone, silt
6755'	Laminated silt (light-medium gray)
6763'	Silt (black, structureless)
6767'	Silt and sandstone (micro, laminations)

Table 1. Core samples selected for point load test.

Given the finely-laminated nature of the lower Brushy Canyon siltstones and sandstones, some of the samples were considered anisotropic, and were tested according to the procedure and recommendations under *Anisotropic rock*, ISRM: Point Load Test publication (Franklin, 1985). According to the recommendations, a sample should be tested in directions which give the greatest strength values, generally parallel to the planes of anisotropy (bedding or lamination planes). For these samples, the load was applied along, or parallel, to the planes of anisotropy as shown in Figure 4. For samples with no apparent bedding or lamination planes the load was also applied in the same direction, or perpendicular to the core axis.

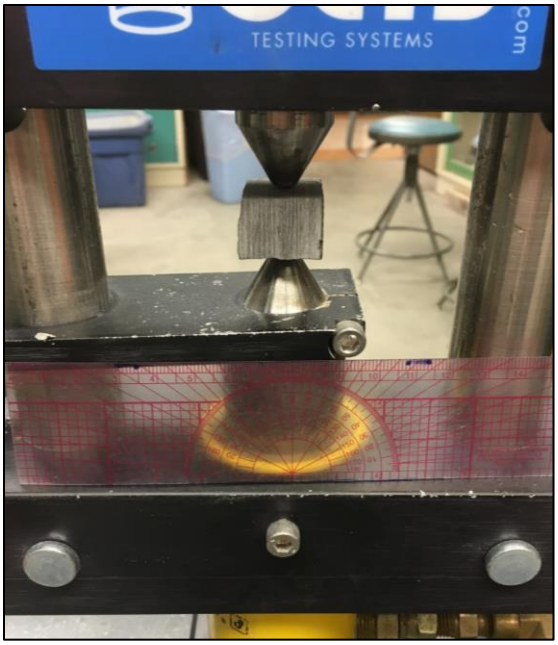

Fig. 4 Pre-test photo of finely-laminated siltstone sample (depth 6755') held in place by two load platens. Load is applied parallel to the planes of anisotropy (laminations).

Point Load Test. The point load strength test was used to determine the fracture toughness for different lithologies from the #23 core. The point load test is used as an index test for the strength classification of rock materials, and may also be used to predict uniaxial tensile and compressive strength parameters, as well as fracture toughness (Franklin, 1985). The point load testing apparatus is designed to induce tensile stress into a rock sample by the application of a compressive force. Bearman (1999) proposed a method for the rapid estimation of Mode I fracture toughness using the point load apparatus, and notes the correlation between fracture toughness and point load strength, where the force required by the point load apparatus to induce cracking in a rock sample is proportional to the sample's fracture toughness value.

Measurement of fracture toughness. Fracture toughness, K_{IC} values are calculated by:

$$(1) \quad K_{IC} = \frac{26.56\,P}{(WD)^{\frac{3}{4}}}$$

where

D	Diameter of tested sample
P	Force at failure
W	Minimum width of tested sample

Multiple tests were run a similar samples and data averaged according to the Mean value calculation instructions in the ISRM: Point Load Test publication (Franklin, 1985). The average values are shown as measured values in table 2. For comparison, the default values recommended are also listed in table 2. Note, two of the facies, interbedded silt and sandstone facies (Slt) and in the bioturbated sandstone facies (Bioturb SS) are not available in the library of default K_{IC} values. Also, the measured K_{IC} value for sandstone is significantly less (~40%) than the default value. The K_{IC} values for each lithology type calculated from the point load test results were used in the model simulations.

Young's Modulus Values (Mpsi)		
Lithology	*Default*	*measured*
SS	5.00	4.50
LS	1.00	5.32
Slt	N/A	4.50
Bioturb	N/A	4.25
Poisson's Ratio Values		
Lithology	*Default*	*measured*
SS	0.20	0.26
LS	0.30	0.27
Slt	N/A	0.24
Bioturb	N/A	0.24
Stress Gradient Values (psi/ft)		
Lithology	*Default*	*Measured*
SS	0.62	0.57
LS	0.68	0.59
Slt	N/A	0.54
Bioturb	N/A	0.56
Fracture Toughness Values (psi*in$^{1/2}$)		
Lithology	*Default*	*meaured*
SS	1000	596
LS	500	N/A
Slt	N/A	982
Bioturb	N/A	1027.1

Table 2. Software-derived default values and measured rock mechanical property values for each lithology modeled in the simulations. [Fracture toughness from point load tests, young's modulus, Poisson's ratio and stress gradient values from mechanical properties log]

Also shown in table 2 are values of Young's Modulus, Poisson's Ratio and stress gradient derived from log measurements. The mechanical properties log was a critical data source and used extensively for the simulation. The mechanical properties log used sonic and PE curves to calculate and generate Young's Modulus (Mpsi), Poisson's Ratio, and stress gradient (psi/ft) curves every 2 feet between 6500'-6950', across

the productive/perforated zones. Measured versus default Young's Modulus values for limestone (LS) vary by a large gap, 5.32 Mpsi and 1.00 Mpsi, respectively. Actual and default Poisson's Ratio and Stress Gradient values are mostly in agreement. For Poisson's Ratio, the largest difference is ~23% for the sandstone (SS) lithology, and lowest is ~10% difference for the limestone (LS) lithology.

Lithologic Controls on $K_{IC.}$ According to the results above, it appears that K_{IC} values for the reservoir are a function of (1) lithology and (2) sedimentary structure(s). The samples with heterogeneous lithologies (e.g. interbedded silt and sandstone, bioturbated sandstone and siltstone) have the highest K_{IC} values of the sample set, while more homogeneous samples (e.g. clean sandstone, black silt) have lower K_{IC} values. This may be due to an inherent particle or grain size difference between sand and silt. By definition, the grain-size scale for sand particles is 0.0625-2.0 mm, and silt particles is 0.0039-0.0625 mm (Udden, 1898). The silt and sands of the #23 core have been described accordingly, and the descriptions in this work are mostly consistent with descriptions of the work of Justman (2001). How does this grain size heterogeneity affect Mode I fracture toughness (K_{IC})? A recent study evaluated the effects of grain size on fracture toughness and failure mechanism for rocks with similar mineralogical compositions (Sabri, Ghazvinian, & Nejati, 2016). Although their findings show a nonlinear relationship between fracture toughness values of the tested specimens and grain size, specimens with grain size 2-3mm (sand- to small gravel-sized particles) had the highest Mode I fracture toughness values.

Sedimentary Structure Controls on $K_{IC.}$ Sedimentary structures also appear to influence K_{IC} values. The term 'sedimentary structure' refers to the visible features in sedimentary rock that reflect the environmental processes, conditions, and energy levels at the time or near the time of deposition, including laminated bedding, channels, ripple marks, and mudcracks (Boggs, 2006). Samples with high K_{IC} values display one or more sedimentary structures, including finely- and micro-laminated silt and sand, and bioturbation. Samples with few to no sedimentary structures (e.g. Clean SS and Black Slt) have low K_{IC} values. One explanation for this behavior is that certain sedimentary structures and their depositional environment control the distribution of grain type and size within a deposit. For example, laminated bedding is produced as a result of short-lived changes in sedimentation conditions, creating variations in grain size, clay and organic content, and mineral composition (Boggs, 2006). The alternating sand-silt laminae (e.g. MicroLam Slt, Slt SS intlam) in the #23 core created vertical heterogeneity within certain intervals. Conversely, the massive (structureless) sandstone bedding lacks any internal structures, or at minimum, contain faintly developed structures, appearing homogenous in composition, grain size and sorting.

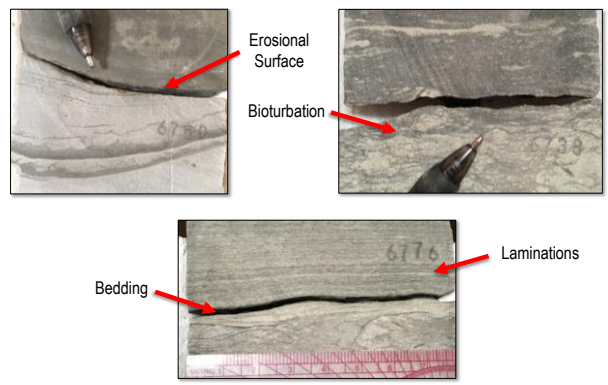

Fig 5. Examples of sedimentary structures and preferential fractures

Preferential Fractures. While describing and measuring the core slabs, numerous locations of broken or fractured core was observed, and appear to have occurred preferentially along boundaries of differing lithologies and within finely-laminated rock. These numerous interbedded and interlaminated sandstone-siltstone sequences create the complex vertical anisotropy in the lower Brushy Canyon Formation. In anisotropic rock, the cracks and flaws are thought to be oriented preferentially along bedding planes (Hoek, 1964). This best explains the behavior mechanism for the preferential fracturing observed in the highly laminated, vertically anisotropic rock of the lower Brushy Canyon Formation. This preferential fracturing behavior is further exaggerated in the formation by the existence of hundreds to thousands of silt-sand laminations sequences.

Single Lithology Model. Geologic models for the Brushy Canyon well varied from assuming a single-layer, homogeneous reservoir described by simplified, average petrophysical properties and default mechanical values to a multi-layered, heterogeneous reservoir with detailed petrophysical properties and measured mechanical values. Single layer, 1-ft, 2-ft, 5-ft and 10-ft models were constructed, but only the single layer and 1-ft models will be discussed in this work. See

Seals, 2016 for more details of all of the models and results. The models were created to compare the results of the hydraulic fracture stimulations using both simplified values and detailed test- and log-derived values. Models were designed to show how variations in layer resolution (multiple layers vs. lumped/averaged layers) affect the simulation results.

The Single Lithology model represents the most "primitive" and least-detailed version of the #23 reservoir. Sandstone was the primary lithology defined, representing a homogenous sandstone reservoir. The model was designed to meet the minimum requirements to simulate a hydraulic fracture: a minimum of three layers must be defined, and the hydraulic fractures must initiate in the middle layers. Corresponding petrophysical properties values were entered for each of the layers.

Detailed Lithology Model. The 1-ft model has the highest layer resolution of the simulated models, containing the highest amount of detail. The reservoir parameters and properties are entered at every 1 foot, with an overlying confining layer designated as sandstone, and an underlying confining layers a limestone. 101 layers were defined, reaching the maximum number of layers allowed by the simulation.

FRACTURE SIMULATION RESULTS

For the fracture modeling phase, the actual treatment volumes, rates and pressures were inputted into the model along with the measured petrophysical and mechanical properties. Model net pressure was matched with the actual values to verify the output. Dimensionless fracture conductivity is a critical design parameter in hydraulic fracture stimulation and subsequent well production analysis that compares the ability of the fracture to transmit fluids into the wellbore with the ability of the formation to deliver fluid into the fracture (Pearson, 2001).

$$(2) \qquad F_{cd} = \frac{k_f w_f}{k l_f}$$

where

k_f	Hydraulic fracture permeability
w_f	Fracture width
k	Average reservoir permeability
l_f	Hydraulic fracture half-length

Figure 6 shows the resulting F_{cd} values for each simulated model using default and measured values. Table 3 details the variables and their respective values used to calculate the F_{cd} values for each model.

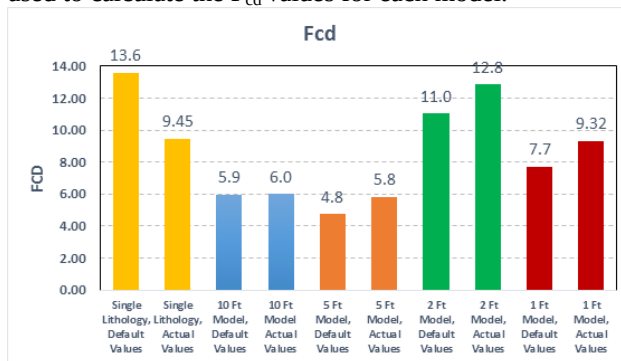

Fig. 6 Dimensionless Fracture Conductivity (F_{cd}) results for all models

The dimensionless fracture conductivity (FCD) from the various models ranged from 4.8 to 13.6. The range depends on the variation of lithofacies included in the fine resolution models and their associated mechanical/petrophysical properties. For example, the resulting average reservoir permeability varies as a function of lithofacies and thus is an artifact of the resolution of the model. The average permeability value for the Single Lithology model, which is comprised of a homogenous sandstone reservoir, is low due to a smaller range of permeability values within the sandstone reservoir layers. The 1-ft model incorporates not only sandstone layers, but siltstones and bioturbated siltstone-sandstone layers, with a wider range of permeability values for each lithology type, resulting in a larger average permeability value of 0.82 mD. As observed in Table 3, an inverse relationship exists between reservoir permeability and FCD as defined by Eq. (2). A second observation is the variation in fracture permeability, from higher values at finer resolution models to decreasing values for coarse (single-layer) models. Subsequently, adding micro-laminated and bioturbated siltstones at the expense of clean sandstone in the finer resolution models resulted in higher permeability, fracture toughness and lower stress gradient.

Model	K_f (mD)	W_f (in)	K (mD)	L_f (ft)	F_{cd}
1-ft Model, Actual Values	0.85	0.49	0.83	537	9.3
1-ft Model, Default Values	0.86	0.47	0.83	625	7.7
2-ft Model, Actual Values	0.88	0.48	0.57	571	12.8
2-ft Model, Default Values	0.87	0.47	0.57	653	11.0
5-ft Model, Actual Values	0.55	0.50	0.80	588	5.8
5-ft Model, Default Values	0.58	0.45	0.80	674	4.8
10-ft Model, Actual Values	0.53	0.50	0.81	546	6.0
10-ft Model, Default Values	0.49	0.53	0.81	538	5.9
Single Lithology, Actual Values	0.51	0.50	0.48	556	9.4
Single Lithology, Default Values	0.695	0.51	0.483	540	13.6

Table 3. Dimensionless fracture conductivity (F_{cd}) variables their respective values for each simulated model

In comparing the 1-ft and Single Lithology models, Actual Values, it appears that 1) use of detailed petrophysical and reservoir properties, or lack thereof, in the reservoir models and 2) layer thickness resolution, either high or low, make a minor difference in the resulting F_{cd} values. However, the use of detailed vs. simplified petrophysical and reservoir parameters for a given model make a significant difference in the hydrocarbon pore volume calculations, which in turn affects the hydrocarbon production values and history matching results.

The hydraulic fracture treatment sand was tagged with multiple radioactive (RA) tracers and a post-hydraulic fracture treatment log run to identify stimulated zones. Unfortunately, wellbore fill omitted the lower perforated "L" zone interval from analysis, and therefore was not included in this work.

The RA tracer log and the proppant concentration profile were juxtaposed to show the correlation between the simulated proppant concentration and the RA-tagged proppant locations along the perforated wellbore. For the 1-ft, measured values model, the RA tracer log and the proppant concentration profile roughly correlate the proppant placement within the reservoir (Figure 7). Starting at the uppermost perforation at 6654' to ~6675', the proppant concentration ranges from 1.8 to 2.1 lb/ft^2. The low proppant concentrations here correspond with low gamma ray and counts-per-second (CPS) values in the RA tracer log. At depths 6675'- 6700', proppant concentrations increase to 2.1- 2.35 lb/ft^2 with increased gamma ray and CPS readings. From depths 6700'- 6740', the proppant concentrations are highest in the RA tracer log and range from 2.4- 2.8 lb/ft^2. Depth 6740' has the highest proppant concentration values of 2.7 lb/ft^2 and higher, yet the RA tracer log does not necessarily reflect this increase in proppant at this depth.

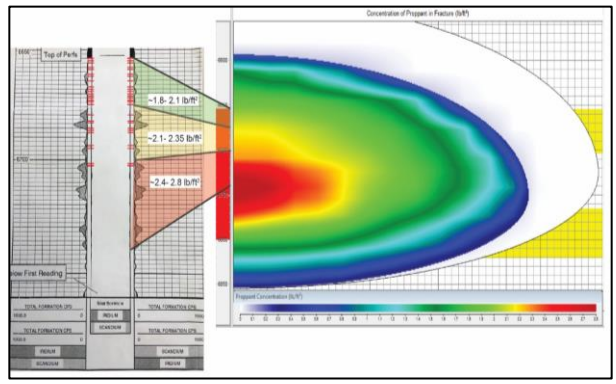

Fig. 7 RA tracer log and simulated proppant concentration profile along the perforated wellbore for 1-ft, Actual Values model. Red bars marks in tracer log represent the "K" zone perforations.

The proppant concentration profile for the single lithology, actual values model is shown in Figure 8. Unlike the 1-ft Actual Values model (Fig. 7), the proppant concentration gradient from low to high values is not well-defined and stratified. From 6654'- 6670', the proppant concentration ranges from ~1.8- 1.9 lb/ft^2, and abruptly increases to 2.2 lb/ft^2 and 2.35 lb/ft^2 at depth 6670'. At this depth, the RA tracer log indicates the proppant concentration values should range between 2.1- 2.35 lb/ft^2. This discrepancy between the results indicate that the over-simplified and homogenous sandstone reservoir model does not contain the reservoir properties or detailed layer resolution that would allow for accurate simulated hydraulic fracture behavior that represents actual fracture behavior. The roughly positive correlation between the RA tracer log and proppant concentration profile for the 1-ft model further validates that the model is the most appropriate for use in the hydraulic fracture simulations.

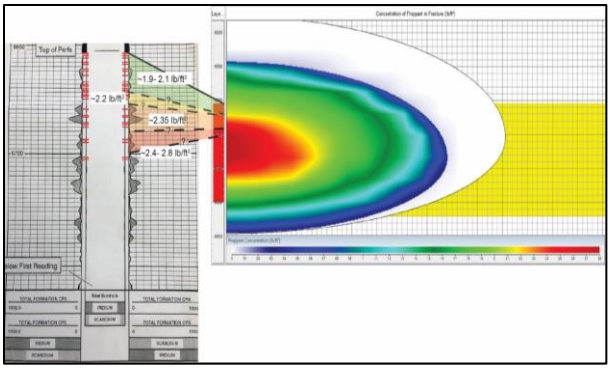

Fig. 8 RA tracer log and simulated proppant concentration profile along the perforated wellbore for Single Lithology, Actual Values model. Red tick marks in the tracer log represent the "K" zone perforations.

PRODUCTION HISTORY MATCHING

Actual well production and pressure history was used to compare the results of fracture stimulation modelling efforts. For each simulation, production rate was constrained, and pressure was the matching variable. Results are shown in Figure 9 for four cases, single-layer vs 1-ft fine resolution model and actual vs default mechanical properties.

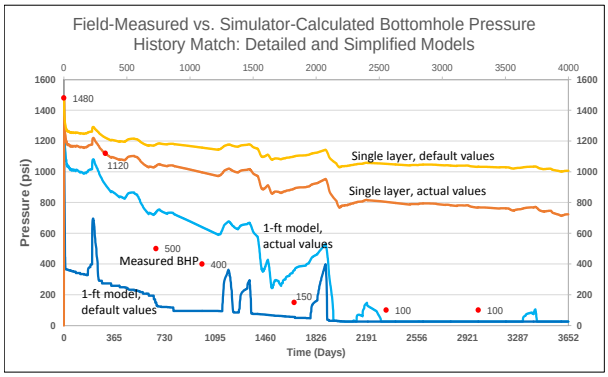

Fig. 9 Simulator-calculated bottomhole pressure for various model resolutions and input mechanical properties compared to field-measured bottomhole pressure data

As seen in the figure, a pressure match was not achieved for the simplified, homogenous lithology model. This behavior is due to the simulator over estimating reservoir volume based on calculated net pay values. For the single lithology, actual values model, the net pay is 167 ft, whereas the 1-ft, actual values model net pay is 104 ft. The simulator over-estimates the 167 ft net pay based off of the specified reservoir parameters for each model, thus over-estimating the hydrocarbon volume in the reservoir.

The pressure match results for the 1-ft models show an improvement in estimating bottomhole pressure, with the 1-ft, actual values model the best estimate. The use of default petrophysical values, even when used in conjunction with detailed, high-resolution reservoir layers, is insufficient for achieving a production history match.

Although the F_{cd} values for each model are similar (9.45 for single lithology vs 9.32 for 1-ft model both using actual values), the 1-ft model better represents the Well #23 reservoir and fracture characteristics. The difference is the OOIP values vary greatly between the two models. The Single Lithology model OOIP value (1235 Mbbls) indicates a very large hydrocarbon pore volume, and the lack of pressure drop after early-time production doesn't allow for a match with the field-measured bottomhole pressure (BHP). The production pressure drop for the 1-ft, Actual Values model occurs early on, and reflects a much smaller hydrocarbon pore volume, 471 Mbbls.

CONCLUSIONS

Modeling hydraulic fracture behavior using simplified reservoir parameters result in consistently over- or under-estimated fracture parameters and ultimately affect simulated production behavior. The use of detailed vs. simplified layers for a given model makes a significant difference in the hydrocarbon pore volume calculations, which affects the BHP and production history matching results. As layer thickness resolution increases from simplified to detailed (e.g. from one lumped layer to 1-ft increments), hydrocarbon pore volume decreases, resulting in a more accurate pressure match.

The degree of detail in layer thickness resolution, lithologic representation, and the use of software-default versus actual petrophysical values affect the resultant production behavior. Using measured mechanical properties values in simulations provide the best representation of the hydraulic fracture simulation over generic or program default values for a given lithology.

ACKNOWLEDGEMENTS

The authors wish to thank Strata Production Co. for providing the well data necessary to verify this work. They would also like to thank FRACPRO™ and Digital Formation for providing students access to their software.

REFERENCES

Bearman, R. A. (1999). The use of the point load test for the rapid estimation of mode I fracture toughness. International Journal of Rock Mechanics and Mining Sciences, 36(2), 257-263.

Boggs, J., Sam. (2006). Principles of sedimentology and stratigraphy (4th ed.): Prentice Hall.

Franklin, J. (1985). Suggested method for determining point load strength. Paper presented at the International Journal of Rock Mechanics and Mining Sciences & Geomechanics Abstracts.

Hoek, E. (1964). Fracture of anisotropic rock. Journal of the South African Institute of Mining and Metallurgy, 64(10), 501-523.

Justman, H. (2001). Petroleum source rocks in the Brushy Canyon Formation (Permian). Delaware Basin, southeastern New Mexico: MS thesis, Earth and Environmental Sciences Department, New Mexico Institute of Mining and Technology.

Pearson, C. M. (2001). Dimensionless fracture conductivity: better input values make better wells. Journal of petroleum technology, 53(01), 59-63.

Sabri, M., Ghazvinian, A., & Nejati, H. R. (2016). Effect of particle size heterogeneity on fracture toughness and failure mechanism of rocks. International Journal of Rock Mechanics and Mining Sciences, 81, 79-85.

Scott, G., & Carrasco, A. (1996). Delaware sandstone reservoir completions and real-time monitoring of hydraulic fractures. Publications-Society of Economic Palaeontogogists and Mineralogists, Permian Basin Secion SEPM, 183-188.

Seals, K. (2016) MS thesis, Impact of petrophysical properties on hydraulic fracture analysis, Petroleum Engineering Department, New Mexico Institute of Mining and Technology

U.S. Department of Energy, E. I. A., Independent statistics & analysis. (2016). Trends in U.S. Oil and Natural Gas Upstream Costs. 141.

Udden, J. A. (1898). The Mechanical composition of wind deposits: Lutheran Augustana book concern, printers.

ABOUT THE AUTHORS

Kelsey Seals graduated with a B.S. degree in Earth Science from New Mexico Tech in 2009, and a M.S. degree in Petroleum Engineering from New Mexico Tech in 2017. Previously she was a GIS Mapping Technician at the New Mexico Bureau of Geology and Mineral Resources, and was employed as both a geology and engineering intern for a small oil company in the Permian Basin. Other research work includes petrographic analysis of fluvial deposits, investigating complex alluvial fan stratigraphy and depositional boundaries, and reservoir characterization and evaluation of formations in the Delaware Basin. She is an active member in numerous professional societies.

Dr. Thomas Engler is Professor of Petroleum Engineering at New Mexico Tech. Previously he was a faculty member at the University of Tulsa, and was a reservoir/production engineer with over nine years of experience in the oil and gas industry primarily in the Permian Basin and Rocky Mountain regions.

Dr.Engler graduated with B.S. degrees in Geology and Petroleum Engineering from New Mexico Tech in 1980 and 1982, a M.S. degree in Petroleum Engineering from New Mexico Tech in 1992 and a Ph.D. in Petroleum Engineering from the University of Oklahoma in 1995.

Dr. Engler has written numerous articles in areas of reservoir characterization and unconventional gas recovery. Current research interests include coupling formation evaluation with stimulation evaluation, optimization and design. He is a registered professional engineer and an active member in multiple professional societies.